Acta Physiol Plant (2014) 36:3345–3349
DOI 10.1007/s11738-014-1695-5

SHORT COMMUNICATION

Virus interference with trans-plasma membrane activity in infected grapevine leaves

Enrico Rinaldelli · Andrea Luvisi · Alessandra Panattoni

Received: 5 November 2013 / Revised: 26 August 2014 / Accepted: 24 September 2014 / Published online: 2 October 2014

Abstract The trans-plasma membrane behavior in virus-infected grapevine leaves was investigated and the effects of six viruses included in European and Italian certification protocols of grapevine on trans-plasma membrane potential (t-PMEP) or electron transport (t-PMET) activity were evaluated. Electrophysiological tests were carried out on leaf samples of virus-infected *Vitis vinifera* cv. Sangiovese. Microelectrodes were placed in the central zone of the mesophyll for membrane potential measurement, while carbon fiber microelectrodes were used to estimate the membrane reductase activity of virus-infected resting cells. Viruses, the presence of which increased the NADH content, interfere differently with t-PMEP and t-PMET. Those that did not interfere negatively with membrane potential caused an increment in cell reductase activity, while virus-infected samples which showed a stressed status—as suggested by low energy availability and difficulty in the impalement procedure—were characterized by a lower t-PMET activity despite NADH content.

Keywords t-PMEP · t-PMET · GLRaV-1 · GLRaV-3 · NADH

Communicated by E. Kuzniak-Gebarowska.

E. Rinaldelli
Department of Agrifood Production and Environmental Sciences, Section Arboriculture, Laboratory of Electrophysiology, University of Florence, Viale delle Idee, 30, 50019 Sesto Fiorentino, Florence, Italy

A. Luvisi · A. Panattoni (✉)
Department of Agriculture, Food and Environment, University of Pisa, Via del Borghetto, 80, 56124 Pisa, Italy
e-mail: alessandra.panattoni@unipi.it

Introduction

Cell plasma membranes have signaling systems for regulating a variety of biological functions, including cell metabolism, proton pumping, activity of ion channels, growth, death and defense mechanism by pathogens (Ly and Lawen 2003). In the literature regarding human virus diseases, many studies have been conducted describing events related to virus infection assessment and related variation in plasma membrane potential (Akeson et al. 1992; Helenius et al. 1985; Wiley and Skedel 1987) and it has been speculated that observed depolarization could be related to alteration of selective ion channels responsible for variation in membrane potential linked to virus-host interaction. In plants, plasma membrane H^+-ATPases are dynamically regulated during plant immune responses and recent quantitative proteomics studies suggest complex spatial and temporal modulation of plasma membrane H^+-ATPase activity during early pathogen recognition events (Elmore and Coaker 2011).

With regard to plant virus research, very few data are available on membrane behavior during phytovirus infection. The first time that changes of membrane electropotentials were characterized during a plant–virus interaction dates back to 1978, in a study by Stack and Tattar (1978) conducted on *Vigna sinensis* infected by Tobacco ringspot virus. In 1997, Schvarzstein conducted a study on *Gomphrena globosa* infected by *Papaya mosaic virus* and *Tobacco mosaic virus*. The author observed changes in average ion currents, identifying an early event in the signal transduction pathway related to virus–host interaction. In 1982, Novacky and Ullrich-Eberius (1982) reported a similar interaction in cotton plants infected by *Xanthomonas campestris*. Shabala et al. (2010) called attention to this topic with a study on ion fluxes across cellular

membranes during virus infection processes in tobacco, potato, periwinkle and sugar beet plants infected by *Potato virus X*.

Electrophysiological tests carried out on leaves of in vitro grapevine explants naturally infected by *Grapevine leafroll-associated virus 1* (GLRaV-1), as well as virus-free explants, showed how virus infection did not cause differences in trans-plasma membrane potential (t-PMEP) activity during antiviral drugs treatments (Luvisi et al. 2012). Differently, in antiviral drug tests conducted on CMV-infected tobacco plants, t-PMEP activity seemed to be influenced by virus presence, acting differently in infected or healthy samples during MPA uptake by cells (Rinaldelli et al. 2012). With regard to trans-plasma membrane electron transport (t-PMET), the elevated activity measured in virus-infected samples (GLRaV-1 and -3) compared to healthy ones indicates that viruses can interfere with the redox homeostasis (Panattoni et al. 2013). These data suggest a possible interaction between virus infection conditions and host trans-plasma membrane activity.

The aim of this study is to investigate the trans-plasma membrane behavior in virus-infected grapevine leaves, evaluating the effects of six viruses included in European or Italian certification protocols of grapevine (2005/43/CE, D.M. 24/06/2008) on t-PMEP and t-PMET activity.

Materials and methods

Plant material

Field-grown *Vitis vinifera* cv Sangiovese infected by *Grapevine fanleaf nepovirus* (GFLV), *Grapevine fleck maculavirus* (GFkV), *Grapevine leafroll ampelovirus 1* (GLRaV-1), *Grapevine leafroll ampelovirus 3* (GLRaV-3) and *Arabis mosaic virus* (ArMV) (viruses included in European Commission directive 2005/43/EC) and *Grapevine vitivirus A* (GVA) (virus included in Italian Ministry Decree D.M. 24/06/2008) were used for t-PMET and t-PMEP trials. The sanitary condition of each plant was confirmed by RT-PCR (Nakaune and Nakano 2006). In June 2013, fully expanded leaves were excised and fresh freehand samples (3–5 mm) were cut with an ethanol-cleaned razor blade for testing (Rinaldelli et al. 2012).

Trans-plasma membrane potential assay

After preincubation for 1 h in basal solution (BS) (Panattoni et al. 2013) adjusted to pH 5.6 with TRIS (2-Amino-2-hydroxymethyl-propane-1,3-diol), leaf segments were prepared according to Luvisi et al. (2012). Continuously aerated BS solution was permitted to perfuse through the chamber at a flow rate of 10.0×10^{-3} L min^{-1}. The measuring electrodes used were micropipettes (tip diameter <1 μm) obtained from single-barreled borosilicate capillaries (World Precision Instruments, Sarasota, USA) as described in Rinaldelli et al. (2012). Insertion of the microelectrodes took place in the central zone of the mesophyll by way of a micromanipulator. Successful microelectrode impalement was determined by the number of cell impalement attempts needed to achieve the stabilization of membrane potential for 5 min (Ober and Sharp 2003). Membrane signal steadiness was calculated considering number of tentative cell impalements out of 15 successful ones. Preincubation and electrophysiological tests were carried out at 22 °C (±0.5) under light (30 W m^{-2}). All tests were conducted on 15 healthy or infected samples. Plots reported were representative of 15 equivalent experiments. Measurements were performed under Faraday cage.

Trans-plasma membrane electron transport assay

For the amperometric measurements, carbon fiber microelectrodes (CFME) (tip diameter 5 μm) (Carbostar-1, Kation Scientific—USA) were used following Rinaldelli et al. (2012). CFME were used in subsequent calibrations to test the linear response in the presence of the redox intermediary. Electrodes were placed in recording solution (RS) with a constant background of 5×10^{-4} M potassium ferricyanide ($K_3[Fe(CN)_6]$) (PF) adjusted to pH 5.6 by MES (2-(N-Morpholino) ethanesulfonic acid), and varying concentrations of potassium ferrocyanide ($K_4[Fe(CN)_6]$) (0, 20, 50, 100 μM). The oxidation current at an electrode potential of +400 mV was measured for each potassium ferrocyanide concentration. Calibration curves were used to estimate the cell reductase activity expressed as [Fe^{2+}] using oxidation current values before each treatment (Rinaldelli et al. 2012). In maize roots, the optimal CFME position from root surface was established at 5 μm (Taylor and Chow 2001). Thus, in this study, the reductase activity was mapped considering the distance of CFME from the leaf cutting surface of healthy plants, starting from position beyond leaf diffusion to the surface.

Sample preparation and reductase activity detection were performed following Rinaldelli et al. (2012). The leaf sample was maintained in RS until the oxidation current stabilized for at least 5 min, and then data were collected. All tests were conducted on 15 healthy or infected samples. Plots reported are representative of 15 equivalent experiments. Measurements were performed under Faraday cage.

NADH assay

NADH was quantified in healthy and infected samples in a colorimetric assay (450 nm) using NADH Quantification

Table 1 Effect of infected status on trans-plasma membrane potential (t-PMEP), signal steadiness, trans-plasma membrane electron transport (t-PMET) and NADH absorbance

Health status	t-PMEP (mV)	Signal steadiness (%)	t-PMET ($[Fe^{2+}]$, μM)		NADH (A_{450})
			5 μm	15 μm	
Healthy	−95.5 ± 9.7b[a]	53.6	47.1 ± 3.7a	42.7 ± 3.2a	0.519 ± 0.061a
GLRaV-1	−95.3 ± 10.3b	51.7	61.3 ± 5.4b	44.0 ± 3.6a	0.730 ± 0.041b
GLRaV-3	−93.7 ± 8.8b	53.6	60.5 ± 4.9b	45.0 ± 5.0a	0.740 ± 0.032b
GFLV	−115.7 ± 10.6c	55.6	59.4 ± 4.6b	43.3 ± 4.6a	0.744 ± 0.089b
ArMV	−112.0 ± 10.4c	50.0	61.1 ± 4.8b	42.7 ± 3.6a	0.725 ± 0.040b
GFkV	−82.0 ± 10.0a	39.5	48.8 ± 3.8a	41.0 ± 3.6a	0.730 ± 0.030b
GVA	−81.6 ± 12.6a	35.7	46.9 ± 5.5a	41.7 ± 4.0a	0.750 ± 0.067b

[a] Values in the same column followed by the same letter do not differ significantly according to Duncan's multiple range test ($P = 0.05$)

Kit (Sigma–Aldrich, St. Louis, MO). All tests were conducted on 15 healthy or infected leaves.

Statistical analysis

Absorbance, $[Fe^{2+}]$ and membrane potential were elaborated using Sigma-Plot software (version 11; Systat Software, San Jose, CA). The software was used to perform two-way analysis of variance (ANOVA) in a random design and pairwise multiple comparisons on significant effects and interactions using the Holm–Sidak method. Data expressed in percent were converted in arcsin values. $P < 0.05$ was considered to be significant. Principal Component Analysis (PCA), a multivariate approach, was performed to evaluate the virus variables.

Results and discussion

Table 1 collects the t-PMEP values. Samples infected by leafroll viruses showed no difference in membrane potential values compared to healthy samples, confirming the similar behavior of leafroll-infected samples and healthy ones observed during antiviral drug treatments (Luvisi et al. 2012). GFLV- or ArMV-infected tissues led to plasma membrane hyperpolarization with higher values compared to healthy samples, while GFkV- and GVA-infected tissues showed plasma membrane depolarization significantly lower than the control. Considering that t-PMEP gradient is generated by H^+-ATPase activity (Sondergaard et al. 2004), GFLV- and ArMV-infected cells could be considered more energized compared to others.

Considering the number of impalements for Em measurements, more attempts were needed for the samples that showed a lower t-PMEP compared to healthy ones, suggesting that GFkV and GVA infection increased the difficulty of cell membrane measurements, as occurs under stress conditions (Vuletic et al. 1987; Rawyler et al. 2002).

With regard to t-PMET, the oxidation current response of the CFMEs was linear with respect to potassium ferrocyanide concentration (in a constant background of 500 μM ferricyanide) in recording solution, as also reported in Rinaldelli et al. (2012). CFME started to oxidize Fe^{2+} at 200 μm from the leaf cutting surface of healthy plants, reaching maximum activity at 5 μm, similarly to the results obtained in maize roots as reported by Taylor and Chow (2001). At 15, 25 and 50 μm the CFME activity was reduced by 8.1, 12.0 and 18.2 %, respectively.

In virus-infected samples (Table 1), at 5 μm-distant CFME readings the $[Fe^{2+}]$ produced by GFkV- and GVA-infected tissues were similar to healthy tissues, while the other infected samples showed a higher t-PMET activity. These differences were lost at the 15 μm-distant CFME reading, probably due to the reduction of CFME activity at the increased distance from leaf cutting surface.

With regard to NADH (Table 1), infected samples showed a significantly higher absorbance at 450 nm compared to healthy samples, confirming results reported in literature for leafroll-infected samples (Panattoni et al. 2013) and extending this behavior to grapevine samples infected by other viruses. In any case, the higher NADH content did not seem to differ in relation to specific infective status.

Considering the PCA performed on the three chosen parameters (Fig. 1), the first principal component axis (PC1) accounted for 60.78 % of the observed variation. It was strongly positively correlated with redox activity and membrane potential, and a positive correlation can be observed for NADH content as well. The second principal component axis (PC2) was strongly correlated with NADH content and negatively correlated with membrane potential. Redox activity was not substantially correlated with PC2. PC1 separated GLRaV-1-, GLRaV-3-, ArMV- and GFLV-infected samples from GFkV-, GVA-infected or healthy samples. PC2 separated all infected samples from GLRaV-1-, GLRaV-3-, GVA- and GFkV-infected samples from

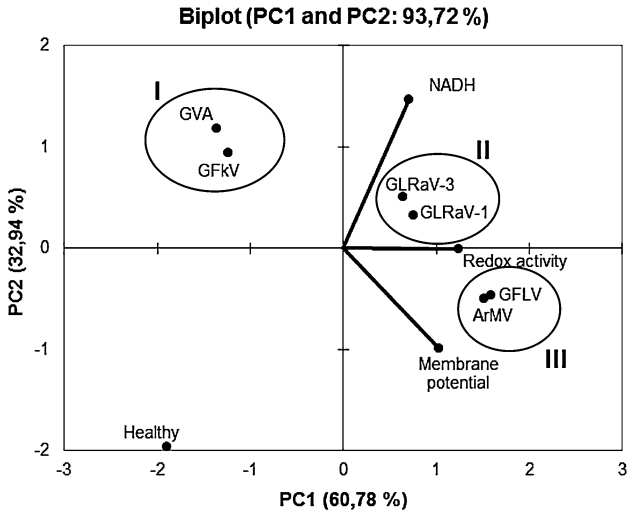

Fig. 1 Biplot of principal component analysis. The length of each eigenvector is proportional to the variance in the data for that element. The angle between eigenvectors represents correlations among different elements. Three groups of elements (*circled*, and denoted I, II and III) show strong positive correlations

ArMV-, GFLV-infected or healthy samples. The biplot shows a strong correlation among GVA- and GFkV-infected samples (group I) as well as among the GLRaVs-infected samples (group II) or ArMV- and GFLV-infected ones (group III). Moreover, considering the chosen variables, healthy samples strongly differ from all infected samples.

Conclusions

Ion fluxes across cellular membranes are known to play a key role in mediating defense mechanisms in plants, and t-PMEP or t-PMET represent signaling systems for regulating cellular metabolism able to interfere with distinct cellular functions such as redox homeostasis and pathogens defense (Herst and Berridge 2006).

In our research, the higher NADH content due to virus infection was used differently by infected samples during their t-PMET activity. Samples whose infectious status did not interfere negatively with membrane potential, such as ArMV, GFLV, GLRaV-1, and -3 showed higher t-PMET activity compared to healthy samples, in agreement with the higher NADH availability. In fact, t-PMET activity involves transport of electrons from intracellular NADH across plasma membrane to an extracellular acceptor, playing a fundamental rule in intracellular redox homeostasis processes strongly linked to the NAD^+/NADH ratio (Del Principe et al. 2011; Gray et al. 2011). Conversely, GFkV- and GVA-infected samples which showed a stressed status, as suggested by the low energy availability and difficulty in the impalement procedure, were characterized by a lower t-PMET activity despite NADH content. All these findings seem to point to an interaction between virus particles and trans-plasma membrane activity, even if not as a homogeneous trend, as shown by PCA analysis. The PCA grouped viruses with similar patterns of effects. The group II of elements included two ampelovirus associated with the grapevine leafroll disease, while the group III of elements included two nepoviruses associated with the complex of infectious degeneration. Thus phylogenetically closely related viruses associated with the same disease seem to show similar electrophysiological patterns of effects. Conversely viruses included in group I of elements, GVA and GFkV, are not phylogenetically closely related. Anyway both viruses do not cause specific symptoms on the foliage of *V. vinifera* (Martelli 2014), leading to patterns of effects similar to those observed in healthy samples. Several points of evidence suggested that, in the early events of the infection process, the viral coat protein may act as an elicitor, compared to an avirulence factor, which is related to host response changes in membrane ion fluxes representing the signal transduction cascade of many plant–virus interactions (Schvarzstein 1997). Moreover, for systemic viruses, movement of viral particles occurs by infected cell to nearby healthy ones, and subsequent systemic transport is governed by a series of mechanisms involving various virus and plant factors. Specialized virus-encoded movement proteins control the transport of viral nucleoprotein through plasmodesmata and their interaction determines the diffusion of the virus (Sholthof 2005). In this way, the virus could interact with the host cell membrane, binding to some cytoskeletal proteins which could include changes in ion fluxes and signal the transduction pathway (Atkinson et al. 1996). Akeson et al. (1992) conducted electrophysiological studies in mammalian cells infected by Vesicular stomatitis virus and suggested that membrane depolarization could block the translocation of nucleocapsid across the epithelial cell plasma membrane during the infection process. Thus, the variety of viral transmembrane proteins should lead to different interactions between viruses and host proteins, acting as an interfering factor of trans-plasma membrane behavior.

Author contribution All authors contributed equally to this work. Enrico Rinaldelli, Andrea Luvisi and Alessandra Panattoni designed and directed the research work. Enrico Rinaldelli, Andrea Luvisi and Alessandra Panattoni performed the experiments and analyzed data. Andrea Luvisi and Alessandra Panattoni prepared the manuscript. Enrico Rinaldelli edited the manuscript. All authors discussed the results and implications and commented on the manuscript at all stages.

Conflict of interest The authors declare that they have no conflict of interest.

References

Akeson M, Scharff J, Sharp CM, Neville DM (1992) Evidence that plasma membrane electrical potential is required for Vesicular Stomatitis Virus infection of MDCK cells: a study using fluorescence measurements through polycarbonate supports. J Membr Biol 125:81–91

Atkinson MM, Midland SL, Keen NT (1996) Syringolide 1 triggers ca^{2+} influx, K' efflux, and extracellular alkalization in soybean cells carrying the disease-resistance gene Rpg4. Plant Physiol 112:297–302

Del Principe D, Avigliano L, Savini I, Catani MV (2011) Trans-plasma membrane electron transport in mammalian: functional significance in healthy and disease. Antioxid Redox Sign 14:2289–2317

Elmore JM, Coaker G (2011) The role of the plasma membrane H^+-ATPase in plant-microbe interactions. Mol Plant 4:416–427

Gray JP, Eisen T, Cline GW, Smith PJS, Heart E (2011) Plasma membrane electron transport in pancreatic B-cells is mediated in part by NQO1. Am J Physiol Endovasc 301:113–121

Helenius A, Kielien M, Wellsteed J, Mellman L, Rudnick G (1985) Effect of monovalent cations on Semliki Forest virus entry into BHK-21 cells. J Biol Chem 260:5691–5697

Herst PM, Berridge MV (2006) Plasma membrane electron transport: a new target for cancer drug development. Curr Mol Med 6:895–904

Luvisi A, Rinaldelli E, Panattoni A, Triolo E (2012) Membrane transport of antiviral drugs in plants: an electrophysiological study in grapevine explants infected by Grapevine leafroll associated virus 1. Acta Physiol Planta 34:2115–2123

Ly JD, Lawen A (2003) Transplasma membrane electron transport: enzymes involved and biological function. Redox Rep 8:3–21

Martelli GP (2014) Directory of virus and virus-like diseases in grapevine and their agents. J Plant Pathol 96S:1–136

Nakaune R, Nakano M (2006) Efficient methods for sample processing and cDNA synthesis by RT-PCR for the detection of grapevine viruses and viroids. J Virol Methods 134:244–249

Novacky A, Ullrich-Eberius CI (1982) Relationship between membrane potential and ATP level in Xanthomonas campestris pv. Malvacearum infected cotton cotyledons. Physiol Plant Pathol 21:237–249

Ober ES, Sharp RE (2003) Electrophysiological responses of maize roots to low water potential: relationship to growth and ABA accumulation. J Exp Bot 54:813–824

Panattoni A, Rinaldelli E, Triolo E, Luvisi A (2013) In vivo inhibition of trans-plasma membrane electron transport by antiviral drugs in grapevine. J Membrane Biol 246:513–518

Rawyler A, Arpagaus S, Braendle R (2002) Impact of oxygen stress and energy availability on membrane stability of plant cells. Ann Bot 90:499–507

Rinaldelli E, Panattoni A, Luvisi A, Triolo E (2012) Effect of mycophenolic acid on trans-plasma membrane electron transport and electric potential in virus-infected plant tissue. Plant Physiol Bioch 60:137–140

Schvarzstein M (1997) Changes in host plasma membrane ion fluxes during the Gomphrena globosa Papaya Mosaic Virus interaction. MSc Thesis, Department of Botany, University of Toronto, Canada

Shabala S, Babourina O, Rengel Z, Nemchinov LG (2010) Non-invasive microelectrode potassium flux measurements as a potential tool for early recognition of virus-host compatibility in plants. Planta 232:807–815

Sholthof H (2005) Plant virus transport: motions of functional equivalence. Trends Plant Sci 10:376–382

Sondergaard TE, Schulz A, Palmgreen MG (2004) Energization of transport processes in plants. Role of the plasma membrane H^+-ATPase. Plant Physiol 136:2475–2482

Stack JP, Tattar TA (1978) Measurement of transmembrane electropotentials of Vigna sinensis leaf cells infected with tobacco ringspot virus. Physiol Plant Pathol 12:173–178

Taylor AR, Chow RH (2001) A microelectrochemical technique to measure trans-plasma membrane electron transport in plant tissue and cells in vivo. Plant Cell Environ 24:749–754

Vuletic M, Radenovic C, Vucinic Z (1987) The role of calcium in the generation of membrane potential oscillations in *Nitella* cells. Gen Physiol Byophis 6:203–207

Wiley DC, Skedel JJ (1987) The structure and function of the hemagglutinin membrane glycoprotein of influenza virus. Annu Rev Biochem 56:365–394